Geophysical Research Letters

RESEARCH LETTER
10.1029/2019GL083400

Liyin He and Zhao-Cheng Zeng contributed equally.

Key Points:
- A mountaintop remote sensing spectrometer is used to derive the time series and spatial pattern of methane emissions in LA basin
- The methane emissions in the LA basin are strongly correlated with the consumption of natural gas by residential and commercial consumers
- About (1.4 ± 0.1)% of the residential and commercial natural gas consumption in LA is released into the atmosphere

Supporting Information:
- Supporting Information S1

Correspondence to:
S. P. Sander,
ssander@jpl.nasa.gov

Citation:
He, L., Zeng, Z.-C., Pongetti, T., Wong, C., Liang, J., Gurney, K. R., et al. (2019). Atmospheric methane emissions correlate with natural gas consumption from residential and commercial sectors in Los Angeles. *Geophysical Research Letters*, *46*. https://doi.org/10.1029/2019GL083400

Received 19 APR 2019
Accepted 10 JUL 2019
Accepted article online 15 JUL 2019

Atmospheric Methane Emissions Correlate With Natural Gas Consumption From Residential and Commercial Sectors in Los Angeles

Liyin He[1], Zhao-Cheng Zeng[1], Thomas J. Pongetti[2], Clare Wong[1,3], Jianming Liang[4], Kevin R. Gurney[4], Sally Newman[1,5], Vineet Yadav[2], Kristal Verhulst[2], Charles E. Miller[2], Riley Duren[2], Christian Frankenberg[1,2], Paul O. Wennberg[1,6], Run-Lie Shia[1], Yuk L. Yung[1,2], and Stanley P. Sander[1,2]

[1]Division of Geological and Planetary Sciences, California Institute of Technology, Pasadena, CA, USA, [2]Jet Propulsion Laboratory, California Institute of Technology, Pasadena, CA, USA, [3]Now at Office of Institutional Research, California State University, Northridge, CA, USA, [4]School of Informatics, Computing, and Cyber Systems, Northern Arizona University, Flagstaff, AZ, USA, [5]Now at Bay Area Air Quality Management District, San Francisco, CA, USA, [6]Division of Engineering and Applied Science, California Institute of Technology, Pasadena, CA, USA

Abstract Legislation in the State of California mandates reductions in emissions of short-lived climate pollutants of 40% from 2013 levels by 2030 for CH_4. Identification of the sector(s) responsible for these emissions and their temporal and spatial variability is a key step in achieving these goals. Here, we determine the emissions of CH_4 in Los Angeles from 2011–2017 using a mountaintop remote sensing mapping spectrometer. We show that the pattern of CH_4 emissions contains both seasonal and nonseasonal contributions. We find that the seasonal component peaks in the winter and is correlated ($R^2 = 0.58$) with utility natural gas consumption from the residential and commercial sectors and not from the industrial and gas-fired power plant sectors. The nonseasonal component is (22.9 ± 1.4) Gg CH_4/month. If the seasonal correlation is causal, about (1.4 ± 0.1)% of the commercial and residential natural gas consumption in Los Angeles is released into the atmosphere.

Plain Language Summary CH_4 is a desirable target for greenhouse gas emission reductions because emission controls will have a rapid impact on radiative forcing. However, its emission budget is highly uncertain and poorly quantified. This paper reports new results from a novel mountaintop remote sensing spectrometer overlooking the Los Angeles basin. The study shows that the megacity's methane emissions are strongly correlated with the consumption of natural gas by residential and commercial consumers, with a leakage rate of (1.4 ± 0.1)%, while the nonseasonal component is (22.9 ± 1.4) Gg CH_4/month. By identifying a clear relationship between CH_4 emissions and natural gas consumption, our results provide strong constraints on the pathways for fugitive CH_4 emissions from the natural gas distribution system in Los Angeles.

1. Introduction

CH_4 accounts for about 25% of the change in radiative forcing total from increases in the well-mixed greenhouse gases (GHGs) since the preindustrial era (Etminan et al., 2016). With an atmospheric lifetime of only about 10 years, CH_4 is a desirable target for GHG emission reductions because emission controls will have a relatively rapid impact on radiative forcing. However, emissions reduction strategies must be tailored to address specific sources, which include landfills, livestock, wastewater treatment, and fugitive emissions from natural gas storage, distribution, and end use equipment.

Legislation in the State of California mandates reductions in emissions of short-lived climate pollutants of 40% from 2013 levels by 2030 for CH_4 (California Legislature, 2006). In the Los Angeles (LA) basin and other urban areas, previous studies focused on methane source attribution have used a variety of methods including C_2H_6 as a tracer for fossil methane, and measurements of CH_4 isotopologues and VOCs to distinguish fossil and biogenic sources (Hopkins et al., 2016; Kuwayama et al., 2019; Wennberg et al., 2012; Wunch et al., 2016). These studies indicate that fugitive natural gas emissions account for 56–70% of the difference between annual top-down and bottom-up (annual excess) CH_4 emissions in LA (Hopkins et al., 2016; Peischl et al., 2013; Wennberg et al., 2012).

Almost all previous studies were restricted in spatial and/or temporal coverage, and none were able to determine which segments and operations of the natural gas distribution system were responsible for the leakage. Wennberg et al. (2012) proposed that many small leaks downstream of the gas meters could be responsible rather than the transport, storage, and distribution segments. Identifying and quantifying the sources of these emissions is critical because methane budgets vary between urban areas, so understanding the emission pathways is essential for mitigation (Jeong et al., 2017; Lamb et al., 2016; McKain et al., 2015).

Recently, we demonstrated a novel remote sensing technique to measure daytime CH_4 emissions in LA from atop Mt Wilson, a mountaintop vantage point (~1,700-m elevation) with nearly unobstructed views of the South Coast Air Basin (SOCAB; Wong et al., 2016). In this method, high-resolution near-infrared spectra are recorded as solar radiation passes through the atmosphere and reflected by the land surface toward the observatory. The instrument points to a series of locations in the SOCAB, providing maps every 90 min of trace gas slant column abundances with a spatial resolution of a few kilometers. Using the tracer-tracer correlation method combined with a highly resolved CO_2 emissions inventory, Wong et al. (2016) showed that it was possible to identify seasonal peaks in spatially aggregated CH_4 emissions in LA. CH_4 emission peaks up to 37 Gg/month were consistently observed in the winter seasons, with a low of 27 Gg/month in the summer. These levels were revised upward in the present study as a result of changes to the underlying CO_2 inventory. Overall, the measured SOCAB CH_4 emissions were 2–31% higher than the scaled statewide bottom-up emissions estimated by the California Air Resources Board (CARB) from 2011–2013 averaged over the three years (CARB, 2011). This result is consistent with other studies that obtained larger emissions than CARB estimates (Conley et al., 2016; Cui et al., 2017; Hedelius et al., 2018; Hsu et al., 2010; Peischl et al., 2013; Wennberg et al., 2012; Wong et al., 2015; Wong et al., 2016; Wunch et al., 2009; Wunch et al., 2016; Yadav et al., 2019). No seasonal variability has been observed in other intensively monitored cities including Indianapolis and Boston although these cities differ significantly from LA in topography, meteorology, infrastructure, and other factors that influence methane emissions (Lamb et al., 2016; McKain et al., 2015).

In the present study, we resolve seasonal and spatial variability of CH_4 emissions from 2011 to 2017 and regress it against consumption data as an important step toward reconciling California's methane budget. The goal of this paper is first to leverage our powerful 2011–2017 data record to quantify seasonal to interannual variability in LA CH_4 emissions. Second, we investigated whether the seasonality of SOCAB CH_4 emissions is related to natural gas consumption. Finally, we quantified the relative contribution of each sector (including residential, commercial, industrial, vehicle, and power plant) to the seasonality of SOCAB CH_4 emissions.

2. Methodology and Data

2.1. Methodology

2.1.1. Observations From CLARS

This study uses GHG slant column abundance data acquired by a Jet Propulsion Laboratory-built Fourier transform spectrometer (FTS) located at the California Laboratory for Atmospheric Remote Sensing (CLARS) on Mt. Wilson overlooking the LA basin at an altitude of 1,673 m above sea level. The instrument design, operating parameters, retrieval algorithms, and measurement approach and performance are discussed in detail in Fu et al. (2014) and Wong et al. (2015, 2016). The daytime measurements have been continuously acquired by CLARS since September 2011. Briefly, CLARS-FTS operates in two observation modes (see supporting information Figure S1): Spectralon Viewing Observations (SVO) and Los Angeles Basin Surveys (LABS). In SVO mode, the FTS points at a Spectralon® plate immediately adjacent to CLARS-FTS. The spectrum is equivalent to a direct solar occultation spectrum in the absence of high clouds. Since CLARS is above the planetary boundary layer (PBL; Ware et al., 2016), the SVO spectra are unaffected by PBL pollution and therefore provide an approximation to background trace gas column densities. In LABS mode, the FTS points sequentially at the 33 surface target sites (see supporting information Figure S2), which span most of the LA Basin. In this mode the reflected radiance traces several kilometers in the

PBL and is therefore very sensitive to GHG emissions. There are five to eight standard measurement cycles per day. In each standard measurement cycle, the FTS observes 33 surface targets and acquires four interspersed SVO measurements, pointing at each target for about 3 min. The sampling time of CLARS depends on the length of the daytime. During summer, CLARS performs eight measurement cycles from ~6 a.m. to ~8 p.m., while during winter, CLARS operates five measurement cycles from ~8 a.m. to ~5 p.m.

Slant column densities (SCDs), the total number of molecules per unit area along the path, of trace gases CO_2, CH_4, and O_2 are retrieved by fitting spectral lines at 1.60, 1.67, and 1.27 μm, respectively (Fu et al., 2014). The slant column averaged dry air mixing ratios of CO_2 (XCO_2) and CH_4 (XCH_4) are calculated as follows:

$$XCO_2 = \frac{SCD_{CO2}}{SCD_{O2}} \times XO_2 \tag{1}$$

$$XCH_4 = \frac{SCD_{CH4}}{SCD_{O2}} \times XO_2 \tag{2}$$

where XO_2 is the mixing ratio of oxygen in air (0.2095).

2.1.2. Monthly Ratio of Excess XCH_4 to Excess XCO_2

As discussed by Wong et al. (2015), data filtering was applied to remove measurements with high aerosol scattering impact, low signal-to-noise ratio, and high solar zenith angles. In addition, measurements were removed when the spectra fitting residuals exceed a predefined threshold (Fu et al., 2014; Wong et al., 2015). Excess XCH_4 (XCH_4xs) and excess XCO_2 (XCO_2xs) are obtained by subtracting the background XCH_4 and XCO_2 acquired using SVO mode from those acquired using LABS mode, respectively (Wong et al., 2016):

$$XCO_{2xs} = XCO_{2LABS} - XCO_{2SVO} \tag{3}$$

$$XCH_{4xs} = XCH_{4LABS} - XCH_{4SVO} \tag{4}$$

Wong et al. (2016) used orthogonal distance regression analysis to quantify monthly XCH_4xs/XCO_2xs correlation slopes for each surface target and then used the weighted average slope across all targets to represent the monthly XCH_4xs/XCO_2xs ratio over the LA Basin. In the orthogonal distance regression analysis, we found that data anomalies may bias the estimated correlation slope, which is important for the determination of emission ratios.

In this work, we derived an unbiased background of XCH_4 and XCO_2 along the same path as CLARS target mode using XCO_{2SVO} and XCH_{4SVO} combined with National Oceanic and Atmospheric Administration in situ flask measurement on Mt. Wilson (see supporting information S1). Also, we used a different approach to derive monthly XCH_4xs/XCO_2xs, which is found to better capture the mean pattern as well as the anomalies. To derive monthly XCH_4xs/XCO_2xs, daily XCH_4xs/XCO_2xs over the LA Basin is first obtained by averaging individual XCH_4xs/XCO_2xs measurements for each surface target. Measurements with XCO_2xs less than 2 ppm are removed to confine the analysis to emissions within the basin, as in Wunch et al. (2009). The time series of XCH_4xs to XCO_2xs ratio including all measurements from CLARS-FTS over all surface targets in the LA basin from 2011 to 2017 is shown in supporting information Figure S3. Monthly XCH_4xs/XCO_2xs can then be computed as the average of the daily ratios over a given month. The corresponding standard error for each month is also calculated. Supporting information Figure S4 shows the seasonal pattern of XCH_4xs/XCO_2xs ratios and the associated errors.

2.1.3. Deriving Top-Down Monthly CH_4 Emissions

Following Wong et al. (2015, 2016), we used the tracer-tracer method (Wunch et al., 2009) to derive the monthly CH_4 emissions based on the estimated monthly XCH_4xs/XCO_2xs ratio in the LA basin:

$$E_{CH4}\Big|_{monthly}^{top-down} = \frac{XCH_{4xs}}{XCO_{2xs}}\Big|_{monthly}^{CLARS} \times E_{CO2}\Big|_{monthly}^{inventory} \times \frac{MW_{CH4}}{MW_{CO2}} \tag{5}$$

where $E_{CO2}\big|_{monthly}^{inventory}$ is CO_2 inventory emissions in the LA Basin. We used the Hestia V2.5 data set in this paper, assuming 10% uncertainty in the inventory data set Gurney et al. (2012) and Gurney et al. (2019)

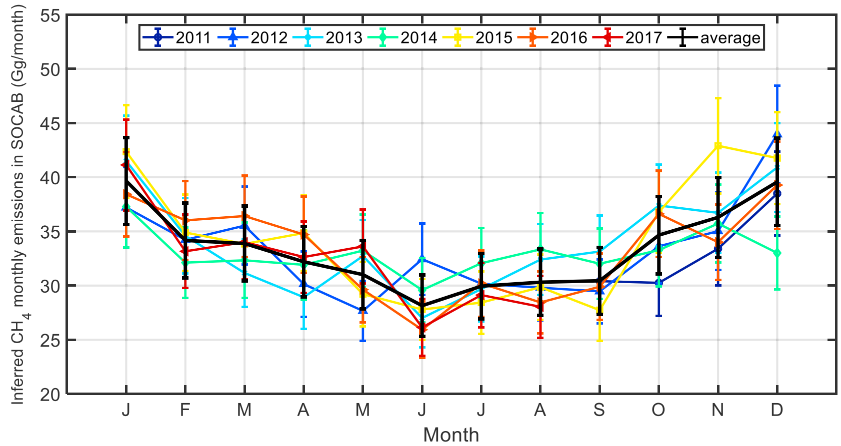

Figure 1. Monthly CH_4 emissions in the Los Angeles basin from September 2011 to December 2017. The monthly average over the measurement period is shown in black. Uncertainties are estimated by error propagation using the uncertainties of monthly patterns of XCH_4xs—XCO2xs (supporting information Figure S4) and the assumption of 10% uncertainties in Hestia CO_2 inventory data (supporting information Figure S9). SOCAB = South Coast Air Basin.

(more details in supporting information S2); $\frac{MW_{CH4}}{MW_{CO2}}$ is the ratio of the molecular mass of CH_4 and CO_2. This tracer-tracer inversion method is built on the strong correlations between CH_4 and CO_2 measured in the PBL in source regions. The XCH_4xs/XCO_2xs ratio has been identified with local emission ratios for the two gases (Wennberg et al., 2012; Wunch et al., 2009). Moreover, the effects of aerosol scattering on the XCH_4xs and XCO_2xs largely cancel out and the impact on their ratio is assumed to be negligible (Zhang et al., 2015). This tracer-tracer method in deriving CH_4 emissions is based on a number of assumptions as discussed in detail by Wong et al. (2016).

2.2. Relative Importance of Different Natural Gas Consumption Sectors in CH_4 Emissions

To determine the relative importance of different natural gas consumption sectors to the monthly CH_4 emissions, we applied a multiple linear regression model (Grömping, 2006) with the averaging over orderings method proposed by Lindeman (1980). The relative importance is obtained by decomposing the model-explained variance into a fixed number of components associated with the contribution of each predictor. In practice, the R package of "relaimpo" (Grömping, 2006) is used to quantify the relative importance of each predictor in the regression model. This method has been widely used in environmental studies (Arrigo et al., 2015; Jones et al., 2014; Wu et al., 2013). In our case, the predictors are the natural gas consumption from several individual sectors, including residential, commercial, industrial, vehicle, and electric power. The dependent variable is the total monthly CH_4 emissions inferred from CLARS data.

2.3. Data

2.3.1. Monthly Natural Gas Consumption Data Set

Natural gas usage data are the sum of natural gas usage data from residential, commercial, industrial, vehicle, and power plant sectors in the SOCAB. The residential, commercial, and industrial data are available publicly on Southern California Gas Company (SoCalGas) database (SoCalGas, 2018). Power plant data are provided by the California Energy Commission online database (California Energy Commission, 2018). The time series of the natural gas consumption of individual sectors are shown in supporting information Figure S7.

2.3.2. Monthly Average Surface Air Temperature

The monthly average surface air temperature data in Los Angeles Downtown/USC, CA (171 meters above sea level) are obtained from the stational data inventory in the National Oceanic and Atmospheric Administration/National Weather Service Cooperative Observer Network (https://wrcc.dri.edu/cgi-bin/cliMAIN.pl?ca5115). All months from September 2011 to December 2016 are used. The surface air temperature in this study is the temperature of the free air conditions surrounding the station at a height between 1 and 2 m above ground level. The air should be freely exposed to sunlight and wind. It is not close to or

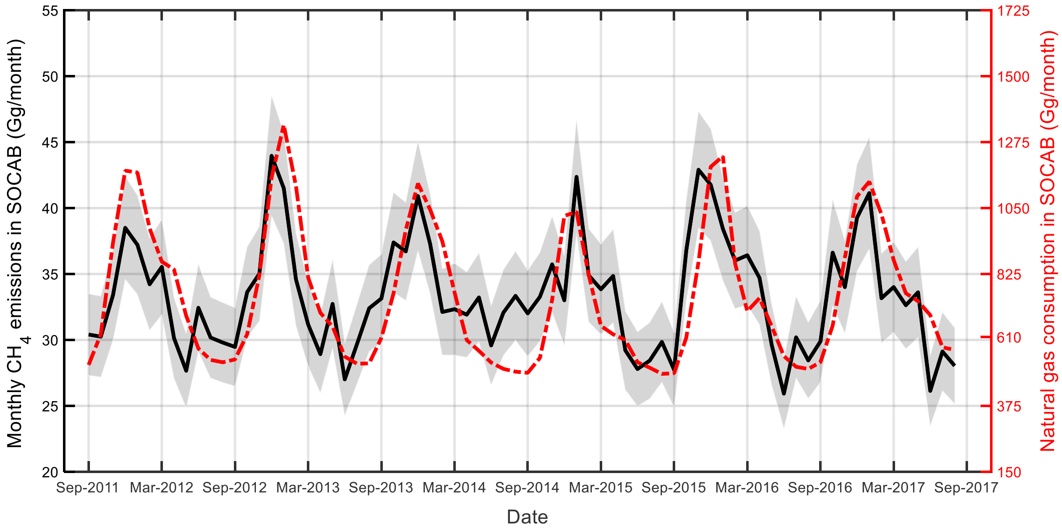

Figure 2. SOCAB CH_4 emissions expressed as a continuous time series (black line, left axis). Monthly natural gas consumption data in the Los Angeles basin from the residential, commercial, and industrial sectors (red dashed line, right axis). The natural gas consumption from the power plant sector does not show significant seasonal variability (supporting information Figure S7). Emissions data from November–December 2015 are impacted by the Aliso Canyon natural gas storage well blowout. SOCAB = South Coast Air Basin.

shielded by trees, buildings, or other obstructions. The temperature data from the observatory are averaged for every 15 s and then averaged to the daily and monthly data.

3. Results

Figure 1 shows the monthly CH_4 emissions in the LA basin from September 2011 to December 2017 along with the monthly average for the observing period overlaid year by year. LA CH_4 emissions exhibit a consistent seasonal pattern, ranging from a minimum of ~27 Gg/month in June–July to a maximum of ~45 Gg/month in December–January. We define the observed difference between measured winter and summer CH_4 emissions as the "seasonal excess" to distinguish it from the annual excess emissions defined above. A spike in emissions in November 2015 coincides with the period of maximum emissions from a very large natural gas storage well blowout at Aliso Canyon that impacted the entire LA basin (Conley et al., 2016). Figure 2 shows the data from Figure 1 represented as a continuous time series, illustrating the prominent winter emissions maxima.

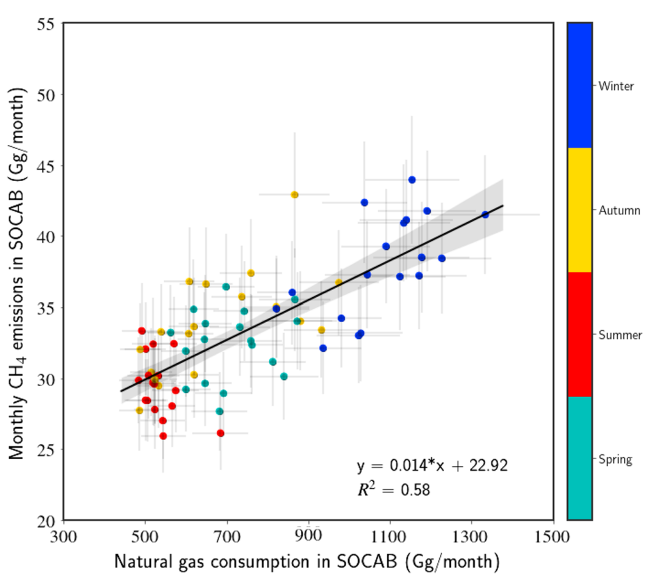

Figure 3. Correlation between derived monthly California Laboratory for Atmospheric Remote Sensing methane emissions and monthly natural gas consumption (residential, commercial and industrial) in the SOCAB from September 2011 to August 2017. Points are color coded by season illustrating the progressive increase in emissions from summer (red) to winter (blue). The correlation that includes power plant consumption is shown in supporting information Figure S12. SOCAB = South Coast Air Basin

As discussed above, multiple previous studies have identified fugitive emissions from natural gas infrastructure as a likely contributor to the observed SOCAB annual excess CH_4 emissions. Figure 2 compares our CH_4 emissions data and monthly natural gas consumption in the SOCAB from the residential, commercial, and industrial sectors as provided by the utility company (see section 2.3). The natural gas consumption data are based on metered customer usage. While the usage data do not include contributions from transmission line leaks, compressor stations, blowdowns, flaring events, and other sources upstream of customer meters, these sources may correlate with metered usage. Figure 2 shows that the observed December–January peaks in monthly CH_4 emissions closely track natural gas consumption.

Figure 3 shows the weighted linear least squares fit between derived monthly CH_4 emissions and natural gas consumption in the SOCAB. The black line is the linear regression weighted by the uncertainties in the derived CH_4 emissions and uncertainties in the consumption data

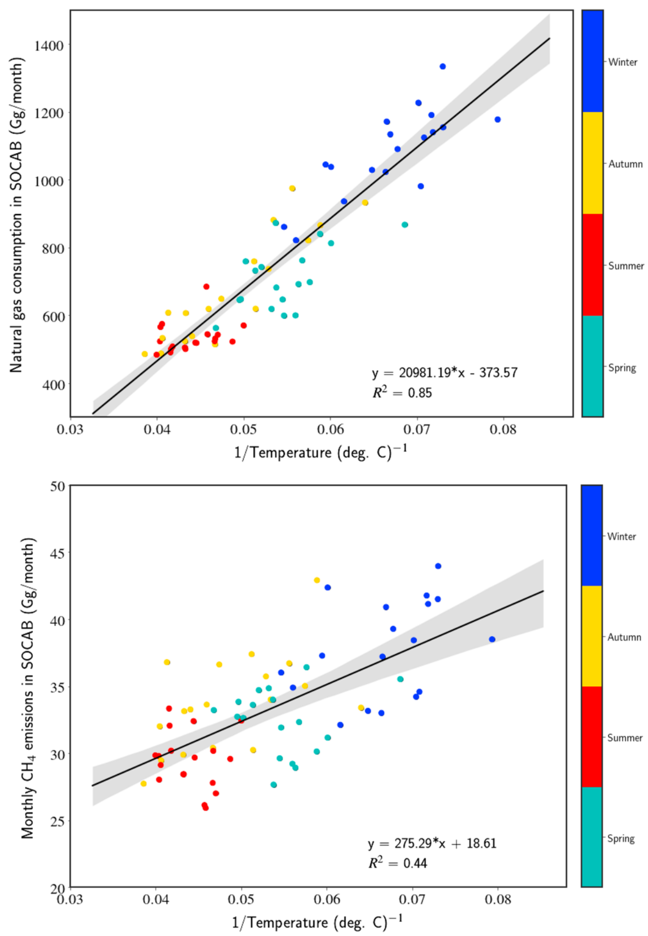

Figure 4. (upper panel) The correlation between monthly natural gas consumption and inverse monthly mean temperature at USC/LA Downtown. (lower panel) The correlation between California Laboratory for Atmospheric Remote Sensing inferred monthly CH_4 emissions and inverse monthly mean temperature at USC/LA Downtown. Increased natural gas consumption for space and water heating at lower ambient temperatures may provide the link to higher observed CH_4 emissions. SOCAB = South Coast Air Basin.

are assumed to be ±10%. The regression slope is 0.0140 ± 0.0014, and the y intercept is 22.9 ± 1.1 Gg/month with $R^2 = 0.58$. We interpret the slope as the fraction of the post-meter natural gas consumption emitted into the atmosphere (from both appliance use and static leaks) while the y intercept gives the CH_4 emissions extrapolated to zero metered consumption, that is, associated with non-metered emissions. The latter would include emissions from landfills, wastewater treatment, local geological sources, and natural gas transmission lines and mains. These sources may have their own seasonality that this simple two-parameter model cannot capture. The fraction of emissions to consumption derived here, (1.4 ± 0.14)%, is somewhat smaller than the range 2.5–6% estimated previously (Wennberg et al., 2012).

The correlation between natural gas consumption and CH_4 emissions may be due to increased wintertime demand by appliances for space heating, water heating, cooking, and other purposes that involve heat generation. To gain further insight into the source sectors responsible for this correlation, we use data on natural gas consumption classified by end use in California from the local utility, SoCalGas, and the California Energy Commission. Monthly data are available for five sectors: residential, commercial, industrial, vehicle fuel, and electric power (see section 2.3 and supporting information Figure S7). Residential and commercial consumption both peak in the winter months, industrial consumption shows small peaks in the summer, while electric power consumption peaks strongly in the late summer (August–September). Consumption by the transportation sector is only a few percent of the total and is not considered. Peaks in industrial consumption are less pronounced and out of phase with residential/commercial usage. A multivariate correlation analysis shows that U.S. Energy Information Administration data for natural gas consumption from the sum of the residential and commercial sectors correlates well (correlation coefficient, $R^2 = 0.89$), while the correlations between industrial consumption and residential/commercial consumption are less evident ($R^2 = 0.23$ and 0.29, respectively).

To quantify the sectoral contributions, the regression equation is given by

$$E_{CH4}\Big|^{\text{top-down}}_{\text{monthly}} = a_0 + a_1\left(NG\Big|^{\text{residential}}_{\text{monthly}} + NG\Big|^{\text{commercial}}_{\text{monthly}}\right) + a_2 \times NG\Big|^{\text{industrial}}_{\text{monthly}} \tag{6}$$

where

E_{CH4} = total monthly excess CH_4 emissions inferred from CLARS data (Gg)
NG_i = reported monthly sectoral natural gas consumption (Gg)
a_i = regression coefficients

The best fit regression coefficients are 27.37, 0.0156, and 0.0094 for a_0, a_1, and a_2, respectively. About 40.4% of the variance between the model and observations is explained by the sum of residential and commercial consumption, and 9.1% is explained by industrial consumption. The results from the regression modeling indicate that there is a strong connection between CH_4 emissions into the atmosphere and residential/commercial natural gas consumption based on time series analysis of both data sets. Taking a_0 as the background excess methane emission in the LA basin, we see that the seasonal component results in a doubling of the total emissions relative to the background. Note that the pattern of emissions must have a seasonal component in order to explain the observations. Quiescent emissions (persistent leaks) from equipment and plumbing cannot explain the strong seasonal signal.

There have been few long-term studies in the SOCAB of CH_4 emissions from the most important sources (natural gas infrastructure, postmeter equipment, landfills, and wastewater treatment plants), providing weak evidence for seasonal variability from these sources (Wong et al., 2016). Only postmeter consumption mimics the observed CH_4 emissions pattern (Wong et al., 2016). Figure 4 shows clear correlations between the inverse of the ambient temperature measured near downtown LA and both natural gas consumption and CH_4 emission rates. Reduced surface air temperatures drive air and water heating demands, resulting in the expected increase in observed CH_4 emissions with decreasing surface temperature (see section 2.3). These observations reinforce the connections between ambient temperature, heating demand and fugitive natural gas emissions. Figure 4 also provides some insight for considering the temperature as an important variable linking natural gas consumptions and CH_4 emissions.

4. Discussion

Since there are no national air quality standards for methane, very little work has been done to characterize the methane emission factors from natural gas-fired appliances such as furnaces, water heaters, stoves, ovens, swimming pool and spa heaters and similar equipment. Currently, the only available emission factor for CH_4 from natural gas-fired furnaces is 5 g/GJ for both commercial and residential furnaces (U.S. Environmental Protection Agency, 2018). From Figure 2, SOCAB winter natural gas consumption surpasses 1,000 Gg/month. Using the Environmental Protection Agency emission factor, this would result in about 0.29-Gg/month seasonal excess methane emissions, which is far less than the observed value of ~20 Gg/month.

There are a number of factors that may close the gap between top-down and bottom-up estimates of seasonal excess methane emissions. Far more research needs to be conducted on emission factors from gas-fired appliances and industrial combustors under different operating conditions (start-up, operation, and shutdown). While increased demand for space heating is clearly associated with lower ambient temperatures in the winter, water heating demand also increases because of decreases in supply water temperature. For example, in the mild, Mediterranean climate of Pasadena, California, measurements from 2001–2016 at six locations showed an average difference of 12 °C in supply water temperature from winter to summer (Kimbrough, 2017). Significantly larger seasonal temperature variability would be expected in colder climates. There is increasing evidence that the probability density functions for CH_4 emissions have a long tail, characterized by a small number of emitters with very large emissions, perhaps due to malfunctioning equipment or improper operating conditions (Zavala-Araiza et al., 2015). This will require a concerted measurement campaign examining large numbers of emitters (thousands) under actual operating conditions targeting residential, commercial, and industrial sectors (Fischer et al., 2018).

5. Conclusions

In conclusion, using mountaintop remote sensing with coverage over the greater LA basin, we observe seasonal excess methane emissions that correlate very well ($R^2 = 0.58$) with combined commercial and residential natural gas consumption. From the covariance we observe that the emissions arise from two terms: one that is seasonally invariant (22.9 $\pm$ 1.1 Gg/month) and another that peaks in the colder months of the year corresponding to (1.4 $\pm$ 0.14)% of residential plus commercial natural gas consumption. Other natural gas consumption sectors (industrial, power plant, and transportation) either have no clear seasonal relationship that matches the observed emissions or are too small. The available emission factor data for residential and commercial natural gas-fired combustion sources fail to explain the observed emissions. Indeed, far more work needs to be done to measure the seasonally varying probability distribution functions of emitters under actual operating conditions.

Acknowledgments
This research was supported by NIST, CARB, and NASA. We gratefully acknowledge discussions with M. Fischer, G. Heath, J. Hedelius, M. Weitz, and V. Camobreco. L.H. thanks the Resnick Sustainability Institute at Caltech for fellowship support. We thank A. Andrews and E. Dlugokencky for providing the NOAA flask measurements at Mt. Wilson Observatory (National Oceanic and Atmospheric Administration, 2019). CLARS-FTS data are available from the NASA Megacities Project (https://megacities.jpl.nasa.gov). The research was carried out at the Jet Propulsion Laboratory, California Institute of Technology, under a contract with the National Aeronautics and Space Administration. L. H., Z. C. Z., T. P., C. W., and S. S. carried out the data acquisition and analysis, J. L. and K. G. provided the Hestia inventory, S. S., L. H., and Z. C. Z. wrote the paper, and all authors contributed to the analysis and discussion of the results. The authors declare no competing financial interests.

References

Arrigo, K. R., van Dijken, G. L., & Strong, A. L. (2015). Environmental controls of marine productivity hot spots around Antarctica. *Journal of Geophysical Research: Oceans*, *120*, 5545–5565. https://doi.org/10.1002/2015JC010888

California Air Resources Board (2011). Greenhouse gas emission inventory—Query tool for years 2000–2011. Retrieved from https://www.arb.ca.gov/app/ghg/2000_2011/ghg_sector.php

California Energy Commission (2018). Online database for power plant statistical information. (Accessed July 23, 2018). https://www.energy.ca.gov/almanac/electricity_data/web_qfer/Power_Plant_Statistical_Information.php

California Legislature (2006). Assembly Bill No. 32. http://www.leginfo.ca.gov/pub/05-06/bill/asm/ab_0001-0050/ab_32_bill_20060927_chaptered.pdf

Conley, S., Franco, G., Faloona, I., Blake, D. R., Peischl, J., & Ryerson, T. B. (2016). Methane emissions from the 2015 Aliso Canyon blowout in Los Angeles, CA. *Science*, *351*(6279), 1317–1320. https://doi.org/10.1126/science.aaf2348

Cui, Y. Y., Brioude, J., Angevine, W. M., Peischl, J., McKeen, S. A., Kim, S. W., et al. (2017). Top-down estimate of methane emissions in California using a mesoscale inverse modeling technique: The San Joaquin Valley. *Journal of Geophysical Research: Atmospheres*, *122*, 3686–3699. https://doi.org/10.1002/2016JD026398

Etminan, M., Myhre, G., Highwood, E. J., & Shine, K. P. (2016). Radiative forcing of carbon dioxide, methane, and nitrous oxide: A significant revision of the methane radiative forcing. *Geophysical Research Letters*, *43*, 12,614–12,623. https://doi.org/10.1002/2016GL071930

Fischer, M. L., Chan, W. R., Delp, W., Jeong, S., Rapp, V., & Zhu, Z. (2018). An estimate of natural gas methane emissions from California Homes. *Environmental Science & Technology*, *52*(17), 10,205–10,213. https://doi.org/10.1021/acs.est.8b03217

Fu, D., Pongetti, T. J., Blavier, J. F., Crawford, T. J., Manatt, K. S., Toon, G. C., et al. (2014). Near-infrared remote sensing of Los Angeles trace gas distributions from a mountaintop site. *Atmospheric Measurement Techniques*, *7*(3), 713–729. https://doi.org/10.5194/amt-7-713-2014

Grömping, U. (2006). Relative importance for linear regression in R: The package relaimpo. *Journal of Statistical Software*, *17*(1), 1–27. https://doi.org/10.18637/jss.v017.i01

Gurney, K. R., Patarasuk, R., Liang, J., Song, Y., O'Keeffe, O., Rao, P., et al. (2019). The hestia fossil fuel CO_2 emissions data product for the Los Angeles Megacity (Hestia-LA). *Earth System Science Data Discussions*, February, 1–38. https://doi.org/10.5194/essd-2018-162

Gurney, K. R., Razlivanov, I., Song, Y., Zhou, Y., Benes, B., & Abdul-Massih, M. (2012). Quantification of fossil fuel CO_2 emissions on the building/street scale for a large US city. *Environmental Science & Technology*, *46*(21), 12,194–12,202. https://doi.org/10.1021/es3011282

Hedelius, J. K., Liu, J., Oda, T., Maksyutov, S., Roehl, C. M., Iraci, L. T., et al. (2018). Southern California megacity CO_2, CH_4, and CO flux estimates using ground-and space-based remote sensing and a Lagrangian model. *Atmospheric Chemistry and Physics*, *18*(22), 16,271–16,291. https://doi.org/10.5194/acp-18-16271-2018

Hopkins, F. M., Kort, E. A., Bush, S. E., Ehleringer, J. R., Lai, C. T., Blake, D. R., & Randerson, J. T. (2016). Spatial patterns and source attribution of urban methane in the Los Angeles Basin. *Journal of Geophysical Research: Atmospheres*, *121*, 2490–2507. https://doi.org/10.1002/2015JD024429

Hsu, Y. K., VanCuren, T., Park, S., Jakober, C., Herner, J., FitzGibbon, M., et al. (2010). Methane emissions inventory verification in southern California. *Atmospheric Environment*, *44*(1), 1–7. https://doi.org/10.1016/j.atmosenv.2009.10.002

Jeong, S., Cui, X., Blake, D. R., Miller, B., Montzka, S. A., Andrews, A., et al. (2017). Estimating methane emissions from biological and fossil-fuel sources in the San Francisco Bay Area. *Geophysical Research Letters*, *44*, 486–495. https://doi.org/10.1002/2016GL071794

Jones, A. K., Jones, D. L., & Cross, P. (2014). The carbon footprint of lamb: Sources of variation and opportunities for mitigation. *Agricultural Systems*, *123*, 97–107. https://doi.org/10.1016/J.AGSY.2013.09.006

Kimbrough, D. E. (2017). Local climate change in Pasadena, Calif., and the impact on streamflow. *Journal-American Water Works Association*, *109*(10), E416–E425. https://doi.org/10.5942/jawwa.2017.109.0114

Kuwayama, T., Charrier-Klobas, J. G., Chen, Y., Vizenor, N. M., Blake, D. R., Pongetti, T., Conley, S. A., Sander, S. P., Croes, B., & Herner, J. D. (2019). Source Apportionment of Ambient Methane Enhancements in Los Angeles, California, To Evaluate Emission Inventory Estimates. *Environmental Science & Technology*, *53*(6), 2961–2970. https://doi.org/10.1021/acs.est.8b02307

Lamb, B. K., Cambaliza, M. O., Davis, K. J., Edburg, S. L., Ferrara, T. W., Floerchinger, C., et al. (2016). Direct and indirect measurements and modeling of methane emissions in Indianapolis, Indiana. *Environmental Science & Technology*, *50*(16), 8910–8917. https://doi.org/10.1021/acs.est.6b01198

Lindeman, R. H. (1980). Introduction to bivariate and multivariate analysis (No. 04; QA278, L553.).

McKain, K., Down, A., Raciti, S. M., Budney, J., Hutyra, L. R., Floerchinger, C., et al. (2015). Methane emissions from natural gas infrastructure and use in the urban region of Boston, Massachusetts. *Proceedings of the National Academy of Sciences*, *112*(7), 1941–1946. https://doi.org/10.1073/pnas.1416261112

National Oceanic and Atmospheric Administration (2019). Earth System Research Laboratory Global Monitoring Division (ESRL GMD) projects at Mt. Wilson Observatory. (Accessed April 8, 2019. http://www.esrl.noaa.gov/gmd/dv/site/MWO.html

Peischl, J., Ryerson, T. B., Brioude, J., Aikin, K. C., Andrews, A. E., Atlas, E., et al. (2013). Quantifying sources of methane using light alkanes in the Los Angeles basin, California. *Journal of Geophysical Research: Atmospheres*, *118*, 4974–4990. https://doi.org/10.1002/jgrd.50413

Southern California Gas Company (2018). Online gas energy usage database (2018). (Accessed June 20, 2018). https://energydatarequest.socalgas.com/

U.S. Environmental Protection Agency (2018). Inventory of U.S. greenhouse gas emissions and sinks. Report No. EPA 430-R-18-003, Annex 2013, Washington, DC. Retrieved from https://www.epa.gov/ghgemissions/inventory-us-greenhouse-gas-emissions-and-sinks-1990-2016

Ware, J., Kort, E. A., DeCola, P., & Duren, R. (2016). Aerosol lidar observations of atmospheric mixing in Los Angeles: Climatology and implications for greenhouse gas observations. *Journal of Geophysical Research: Atmospheres*, *121*, 9862–9878. https://doi.org/10.1002/2016JD024953

Wennberg, P. O., Mui, W., Wunch, D., Kort, E. A., Blake, D. R., Atlas, E. L., et al. (2012). On the sources of methane to the Los Angeles atmosphere. *Environmental Science & Technology*, *46*(17), 9282–9289. https://doi.org/10.1021/es301138y

Wong, C. K., Pongetti, T. J., Oda, T., Rao, P., Gurney, K. R., Newman, S., et al. (2016). Monthly trends of methane emissions in Los Angeles from 2011 to 2015 inferred by CLARS-FTS observations. *Atmospheric Chemistry and Physics*, *16*(20), 13,121–13,130. https://doi.org/10.5194/acp-16-13121-2016

Wong, K. W., Fu, D., Pongetti, T. J., Newman, S., Kort, E. A., Duren, R., et al. (2015). Mapping CH_4: CO_2 ratios in Los Angeles with CLARS-FTS from Mount Wilson, California. *Atmospheric Chemistry and Physics*, *15*(1), 241–252. https://doi.org/10.5194/acp-15-241-2015

Wu, Z., He, H. S., Liang, Y., Cai, L., & Lewis, B. J. (2013). Determining relative contributions of vegetation and topography to burn severity from LANDSAT imagery. *Environmental Management*, *52*(4), 821–836. https://doi.org/10.1007/s00267-013-0128-3

Wunch, D., Toon, G. C., Hedelius, J. K., Vizenor, N., Roehl, C. M., Saad, K. M., et al. (2016). Quantifying the loss of processed natural gas within California's South Coast Air Basin using long-term measurements of ethane and methane. *Atmospheric Chemistry and Physics*, *16*(22), 14,091–14,105. https://doi.org/10.5194/acp-16-14091-2016

Wunch, D., Wennberg, P. O., Toon, G. C., Keppel-Aleks, G., & Yavin, Y. G. (2009). Emissions of greenhouse gases from a North American megacity. *Geophysical Research Letters*, *36*, L15810. https://doi.org/10.1029/2009GL039825

Yadav, V., Duren, R., Mueller, K., Verhulst, K. R., Nehrkorn, T., Kim, J., et al. (2019). Spatio-temporally resolved methane fluxes from the Los Angeles Megacity. *Journal of Geophysical Research: Atmospheres*, *124*, 5117–5130. https://doi.org/10.1029/2018JD029224

Zavala-Araiza, D., Lyon, D., Alvarez, R. A., Palacios, V., Harriss, R., Lan, X., et al. (2015). Toward a functional definition of methane super-emitters: Application to natural gas production sites. *Environmental Science & Technology*, *49*(13), 8167–8174. https://doi.org/10.1021/acs.est.5b00133

Zhang, Q., Natraj, V., Li, K.-F., Shia, R.-L., Fu, D., Pongetti, T. J., et al. (2015). Accounting for aerosol scattering in the CLARS retrieval of column averaged CO_2 mixing ratios. *Journal of Geophysical Research: Atmospheres*, *120*, 7205–7218. https://doi.org/10.1002/2015jd023499

References From the Supporting Information

Tanaka, T., Yates, E., Iraci, L. T., Johnson, M. S., Gore, W., Tadić, J. M., et al. (2016). Two-year comparison of airborne measurements of CO_2 and CH_4 with GOSAT at Railroad Valley, Nevada. *IEEE Transactions on Geoscience and Remote Sensing*, *54*(8), 4367–4375. https://doi.org/10.1109/TGRS.2016.2539973

U.S. Energy Information Administration (2018). Online database for electricity. Accessed May 20, 2018. https://www.eia.gov/electricity/data/state/

Western Regional Climate Center. Climate Historical Summaries. (2019). Online database for Los Angeles DWTN USC campus (Accessed April 8, 2019). https://wrcc.dri.edu/cgi-bin/cliMAIN.pl?ca5115